Available online at www.sciencedirect.com
SCIENCE DIRECT
Journal of Molecular Catalysis A: Chemical 255 (2006) 103–108
JOURNAL OF MOLECULAR CATALYSIS A: CHEMICAL
www.elsevier.com/locate/molcata

The preferential oxidation of CO in excess hydrogen: A study of the influence of KOH/K_2CO_3 on CuO–CeO_{2-x} catalysts

Zhigang Liu, Renxian Zhou *, Xiaoming Zheng

Institute of catalysis, Zhejiang University, Hangzhou 310028, PR China

Received 24 November 2005; received in revised form 1 April 2006; accepted 4 April 2006
Available online 8 May 2006

Abstract

The preferential oxidation of CO in rich hydrogen has been studied for CuO–CeO_{2-x} catalysts. The catalysts were prepared by co-precipitation with K_2CO_3 + KOH as precipitators and characterized using N_2 physisorption isotherms, high resolution transmission electron microscopy (TEM), and X-ray diffraction (XRD). The results indicate that nano-structured CuO–CeO_{2-x} catalysts are obtained, and that the ratio of KOH/K_2CO_3 has a beneficial influence on the properties of CuO–CeO_{2-x} catalysts, i.e., with the addition of KOH, the particle sizes grow smaller, CuO–CeO_{2-x} catalysts have larger surface areas, CuO species in CuO–CeO_{2-x} are more easily reduced and achieve higher catalytic performance in the preferential oxidation of CO in rich hydrogen. CO conversion higher than 99% with O_2 selectivity of 100% is obtained for CuO–CeO_{2-x} catalysts with KOH/K_2CO_3 equal to 4:0 at a temperature of 90–110 °C and a space velocity of 30,000–120,000 ml g^{-1} h^{-1}.

Keywords: Preferential oxidation; CO; Excess hydrogen; CuO–CeO_{2-x}; Precipitator

1. Introduction

Ceria has been widely used in catalytic systems for the elimination of the pollutants contained in the exhaust gases of automobiles [1]. This material contains a high concentration of highly mobile oxygen vacancies, which act as local sources or sinks for oxygen involved in reactions taking place on its surface [2].

Recently, CeO_{2-x} supported CuO catalyst has been attracting attentions because of its activity higher than that of conventional copper-based catalysts and comparable or superior to platinum catalysts for the preferential oxidation of CO in excess hydrogen [3–5]. It is believed that the reaction is catalyzed by the interfacial copper oxide–ceria centers in which ceria presents a high number of oxygen vacancies that permits a high mobility of lattice oxygen [6,7], and the properties of CuO–CeO_{2-x} catalysts have a great dependence on the preparation methods.

For CuO–CeO_{2-x} catalysts, a number of preparation methods have been described, including co-precipitation [8,9], urea-nitrate combustion method [10,11], sol–gel peroxo route [12], etc. CuO–CeO_{2-x} prepared by co-precipitation had been studied by Avgouropoulos et al. [13] and Kim and Cha [14]. The catalysts are prepared with Na_2CO_3 or NaOH solution as precipitators and show superior performance in the preferential oxidation of CO in excess hydrogen at the temperature below 170 °C for a feed of 1% CO, 1% or 1.25% O_2, 50% H_2 in the presence of H_2O and CO_2.

In this work, we prepared the nano-structured CuO–CeO_{2-x} catalysts by co-precipitation with different ratios of KOH/K_2CO_3 as precipitators, and the preferential oxidation properties of CO in rich hydrogen over the catalysts were studied.

2. Experimental

2.1. Catalyst preparation

The CuO–CeO_{2-x} catalysts were prepared by co-precipitating aqueous salt solution of the metal with different ratios of KOH/K_2CO_3 (4:0, 3:1, 2:2, 1:3 and 0:4). The obtained precipitate was washed with de-ionized water to remove residual potassium, and then washed with ethanol before dried at 105 °C for 1 h. The dried samples were thermally treated at 500 °C for about 3 h. Thus, treated catalysts were crushed and sieved to 60–80 meshes. The Cu content in the catalysts was

* Corresponding author. Tel.: +86 571 88273272; fax: +86 571 88273283.
E-mail address: zhourenxian@zju.edu.cn (R. Zhou).

1381-1169/$ – see front matter © 2006 Elsevier B.V. All rights reserved.
doi:10.1016/j.molcata.2006.04.003

expressed as the Cu/(Cu + CeO_2) % weight ratio and all data below were obtained with the 5.0 wt.% Cu catalysts.

2.2. Catalyst characterization

The specific areas of the catalysts were obtained at −196 °C using a Coulter Omnisorp 100CX. Prior to the measurement, the catalysts were pretreated at 250 °C for 2 h. TEM profiles were conducted using a JEOL JEM-2010 (HR) microscope operating at 100 kV. X-ray powder diffraction (XRD) patterns were recorded on a Rigaku D/Max 2550PC powder diffractometer using nickel-filtered Cu Kα radiation. The mean particle diameter was calculated from the X-ray line broadening, according to Scherrer's equation. H_2 temperature-programmed reduction (TPR) was carried out using a conventional reactor equipped with a TCD.

2.3. Catalytic oxidation performance tests

The catalytic performance measurement was carried out in a fixed micro-reactor (quartz glass, 4 mm i.d., 6 mm o.d., length 250 mm) at atmospheric pressure. The reactor temperature was measured by a K-type thermocouple located at the top of the packed catalyst bed and controlled by a temperature controller. The mass of catalyst used in the experiments ranged from 50 to 100 mg, and the catalyst was diluted with inert alumina particles (60–80 meshes) with a dilution ratio of 1:1 by mass. A desired mixture of gases H_2, O_2, CO, CO_2, and Ar was prepared by adjusting the ratio of flows with mass flow controller (Scientific Alicat). The water vapor was introduced with reacting gases bubbling through a heated water bath.

The reactor inlet and outlet streams were measured using an on-line gas chromatograph equipped with a thermal conductivity detector (TCD) and a flame ionization detector (FID). H_2, O_2, CO and CO_2 were separated using a carbon molecular sieve (TDX-01) column. CO and CO_2 were converted to methane by a methanation reactor and analyzed by FID. The detection limit of CO is less than 5 ppm.

Taking into consideration of the existence of CO_2 in feedstock, the CO conversion was calculated based on the CO decrease as follows:

$$\%\ \text{of conversion of CO} = \frac{[\text{CO}]_{\text{in}} - [\text{CO}]_{\text{out}}}{[\text{CO}]_{\text{in}}} \times 100$$

The selectivity is defined as the oxygen consumed by CO oxidation, namely:

$$\%\ \text{of selectivity} = \frac{0.5([\text{CO}]_{\text{in}} - [\text{CO}]_{\text{out}})}{[\text{O}_2]_{\text{in}} - [\text{O}_2]_{\text{out}}} \times 100$$

3. Results and discussion

3.1. Structural studies of $CuO–CeO_{2-x}$ catalysts

The pH values, the surface area, the particle sizes and the temperature required for 50% conversion of CO of $CuO–CeO_{2-x}$ catalysts are listed in Table 1. From Table 1, it can be seen that the addition of KOH results in a decrease in particle sizes from 8.3 to 5.4 nm and increase in pH values from 10.5 to 13.0 and surface area from 40 to 138 $m^2\ g^{-1}$. In addition, when the KOH/K_2CO_3 ratio, λ, increased from 0:4 to 4:0, the oxidation performance of $CuO–CeO_{2-x}$ catalysts is improved greatly; i.e., the reaction temperatures with 50% conversion of CO are lowered from 182.6 to 82.5 °C.

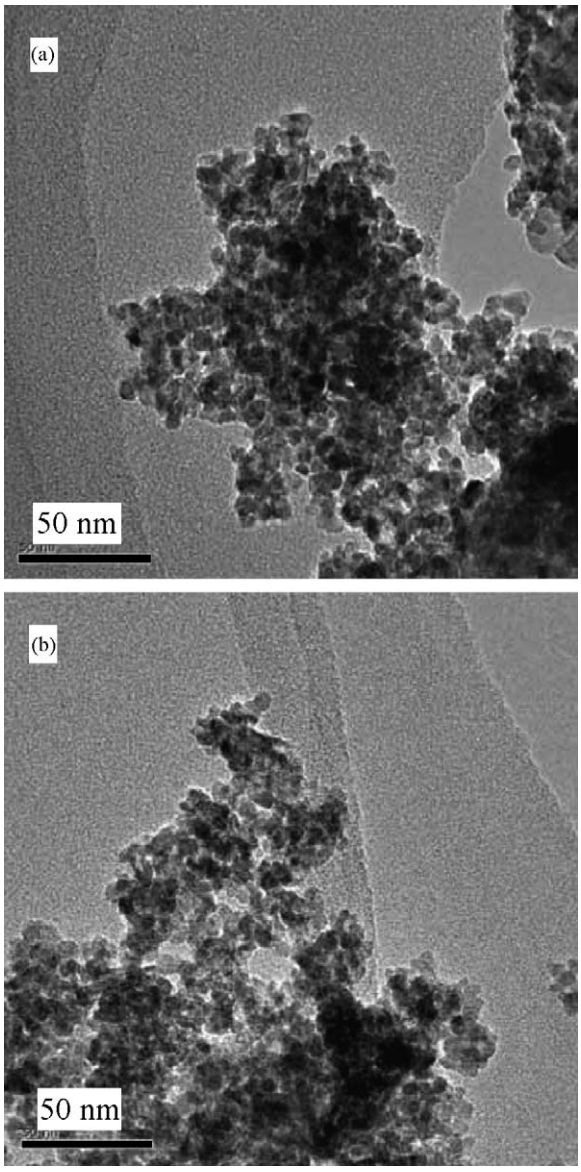

Fig. 1. TEM images of the $CuO–CeO_{2-x}$ catalyst prepared with different of KOH/K_2CO_3: (a) 0:4, (b) 4:0.

TEM images of $CuO–CeO_{2-x}$ catalysts prepared with λ of 0:4 and 4:0, respectively, are presented in Fig. 1. As shown in Fig. 1, the statistical analysis of the dimension of the $CuO–CeO_{2-x}$ particles results in a narrow distribution with a mean diameter around d_{TEM} = 6.5 and 8.5 nm, respectively. In comparison with the data in Table 1, the trend of size variation for both catalysts is similar, though the Scherrer's equation yields slightly lower values for the crystal size than TEM analysis [15].

The XRD patterns of all $CuO–CeO_{2-x}$ catalysts are given in Fig. 2. The distinct fluorite-type oxide structure of CeO_2

Table 1
Characteristics of CuO–CeO_{2-x} catalysts and comparison of their activity in CO oxidation

KOH/K_2CO_3 (molar ratio)	pH	$D_{(1\,1\,1)}$ (nm)[a]	S_{BET} ($m^2\,g^{-1}$)	r_{CO} at 100 °C[b]			T_{50} (°C)[c]
				$mmol_{CO}\,(s^{-1}\,g_{cat}^{-1})$	$mmol_{CO}\,(s^{-1}\,g_{Cu}^{-1})$	$\mu mol_{CO}\,(s^{-1}\,m^{2-1})$	
0:4	10.5	8.3	40	–	–	–	182.6
1:3	11.4	7.9	72	0.2	4.2	5.2	113.0
2:2	12.2	6.9	97	0.7	14.3	7.4	101.0
3:1	12.7	6.2	115	1.2	23.2	10.1	93.0
4:0	13.0	5.4	138	1.4	28.2	10.2	82.5

[a] From line broadening of CeO_2 (1 1 1) peak.
[b] According to literature [7].
[c] W/F = 0.03 g s cm^{-3}.

is present in all catalysts. It can be seen that with decreasing λ value, the peaks of the catalysts become sharper and more intense, corresponding to an increase in size of the crystalline particles. Obviously, the addition of KOH into precipitator inhibits the growth of CeO_2 particles. No observable shift in the diffraction lines of CeO_{2-x} can be found in these catalysts, although Marbán and Fuertes [15] reported that the XRD peaks of CeO_{2-x} are rather broad and shifts of small magnitude might be undetectable. Therefore, it can be concluded that this is dispersed among the ceria crystallites and not forming a true solid solution. CuO_x must be in the form of clusters of XRD amorphous material on the surface of ceria crystals, at least for λ > 0:4, since, as observed in Fig. 3, at λ = 0:4 small but conspicuous diffraction peaks of CuO are detected, meaning that crystallization of CuO starts to occur. It is evident that the addition of K_2CO_3 into precipitator causes the growth of CuO and CeO_{2-x} particles.

3.2. Redox properties of CuO–CeO_{2-x} catalysts

H_2-TPR profiles of CuO–CeO_{2-x} catalysts are shown in Fig. 3 and values of the H_2 consumption and peak temperature maxima are listed in Table 2. From Fig. 3 and Table 2, it can be seen that the curve of CuO–CeO_{2-x} catalyst prepared with λ of 4:0 shows two reduction peaks at 178 and 196 °C, respectively. The peak at 178 °C (called peak α) is ascribed to the copper ions strongly interacting with ceria, and the peak at 196 °C (called peak β) is assigned to the CuO clusters non-associated with ceria [16]. By addition of K_2CO_3 into the precipitator, the hydrogen consumption peaks shift to higher temperatures and the areas of peak α (namely the H_2 consumption) sharply diminish from 22 to 0 $\mu mol/g_{cat}$. When λ = 1:3, it can be seen that peaks α and β coalesce into overlap to one peak and a new peak, called peak γ, appears at 242 °C. According to the results of XRD measurements above, peak γ is assigned to bulk CuO. When λ = 0:4, the peak α vanishes and the H_2-TPR profile of the CuO–CeO_{2-x} catalyst only shows a main peak of hydrogen consumption at 245 °C (peak γ) and a shoulder peak at 227 °C (peak β) in the range of 100–350 °C. It is suggested that the addition of KOH into the precipitator is beneficial to the formation of dispersed CuO_x clusters; however, the addition of K_2CO_3 inhibits this process and yield bulk CuO with a large diameter.

In addition, we find the observed trend in activity with variation of λ values (seen in Table 2) correlates well with that of H_2 consumption of α peak in H_2-TPR of CuO–CeO_{2-x} catalysts. This is in agreement with the proposition [7,17] that

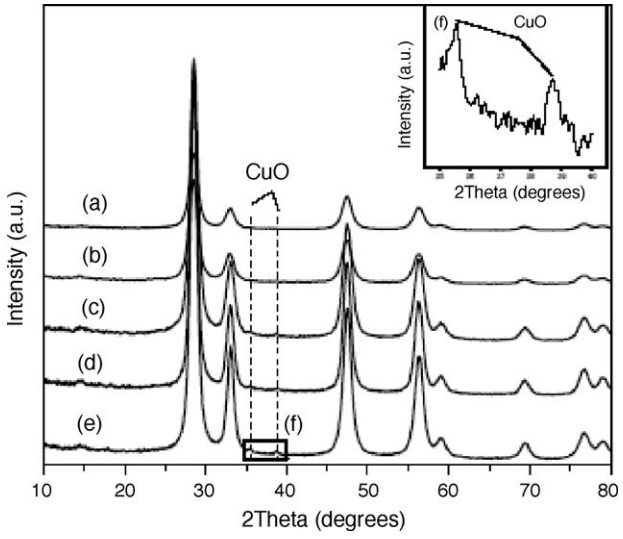

Fig. 2. XRD images of the CuO–CeO_{2-x} catalyst prepared with different ratios of KOH/K_2CO_3: (a) 4:0, (b) 3:1, (c) 2:2, (d) 1:3, (e) 0:4.

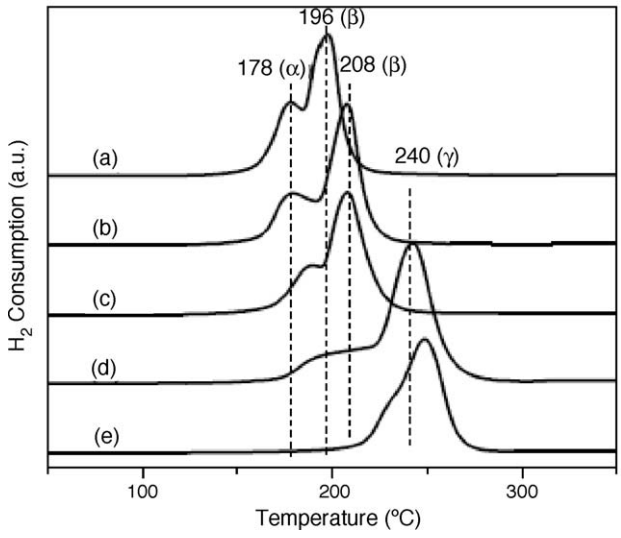

Fig. 3. TPR images of the CuO–CeO_{2-x} catalysts with different ratios of KOH/K_2CO_3: (a) 4:0, (b) 3:1, (c) 2:2, (d) 1:3, (e) 0:4.

Table 2
H_2 consumption and temperature of TPR peaks for catalysts with different λ values

Catalysts (λ values)	α Peak		β Peak		γ Peak	
	H_2 consumption ($\mu mol/g_{cat}$)	Peak temperature (°C)	H_2 consumption ($\mu mol/g_{cat}$)	Peak temperature (°C)	H_2 consumption ($\mu mol/g_{cat}$)	Peak temperature (°C)
4:0	22	176	40	196	–	–
3:1	21	180	45	207	–	–
2:2	13	184	46	208	–	–
1:3	10	197	3	214	42	242
0:4	–	–	16	227	39	245

the high activity of CuO–CeO_{2-x} catalysts is due to the presence of highly dispersed CuO clusters in strongly interacting with CeO_{2-x}, which has a superior reducibility; i.e., the higher reducibility of CuO–CeO_{2-x} catalysts, the higher the catalytic activity. Therefore, the reduction peak α appears at the lowest temperature and possesses the largest H_2 consumption for the catalyst with λ = 4:0 among all catalysts, and the catalyst is most active.

3.3. Oxidation performance of catalysts

The catalytic behavior toward preferential oxidation of CO in rich hydrogen over CuO–CeO_{2-x} catalysts are compared in Fig. 4. The precipitators have an important effect on the catalytic performance of CuO–CeO_{2-x} catalyst. From Fig. 4, it can be seen that the CuO–CeO_{2-x} catalysts prepared with λ of 4:0 shows the highest catalytic activity. Even at 110 °C, CO conversion higher than 99% is observed at a space velocity of 120,000 ml g^{-1} h^{-1} in the absence of CO_2 and H_2O. CuO–CeO_{2-x} catalysts prepared with λ of 1:3, 2:2, and 3:1 achieve the similar conversion of CO at the temperature of 130, 145, 175 °C, respectively, while the CuO–CeO_{2-x} catalyst prepared with λ of 0:4 even cannot achieve the same conversion of CO in the similar temperature range of 70–190 °C. The selectivity of O_2 for CuO–CeO_{2-x} catalysts shows a contrary trend. At low temperature range (lower than 120 °C), the selectivity of O_2 reaches 100%, due to no H_2-oxidation reaction. However, with the increase of reaction temperatures, H_2-oxidation reaction emerges and the selectivity of O_2 decreases with a further increase in the reaction temperature. Arias et al. [18] proposed a reaction scheme, in which Ce^{4+}–O^{2-}–Cu^{2+} pairs are rapidly reduced by CO to produce CO_2. According to these authors CO (and also H_2) molecules are adsorbed on the copper–ceria interfacial region of the catalyst and react with lattice oxygen to produce CO_2 (and H_2O), reducing the copper ion Cu^{2+} to Cu^+. The ceria lattice then supplies the lost oxygen anion to the copper–ceria interface and finally the so formed vacancies are refilled by gaseous oxygen. It is evident that in the above process, the existence on the catalytic surface of relatively higher amounts of easily reducible well dispersed copper oxide species strongly interacting with ceria is the key to the achievement of the superior catalytic performance. This is consistent with the above TPR results.

As for the influence of WGSR (water–gas shift reaction) or reverse WGSR, the catalytic performance of CuO–CeO_{2-x} catalyst prepared with λ of 4:0 in the feed gas of 1% O_2, 8% CO_2, 50% H_2, and argon in balance is also investigated, and the results is illustrated in Fig. 5. From Fig. 5, it is found that the CuO–CeO_{2-x} catalyst is inactive for H_2 oxidation at temperatures up to 150 °C, and the concentration of CO is less than 10 ppm at 165 °C. Liu and Flytzani-Stephanopoulos [7] have also found that the thermodynamic equilibrium constant of the WGSR is at least 25 orders of magnitude lower than the thermodynamic equilibrium constant of CO and H_2 oxidation reactions

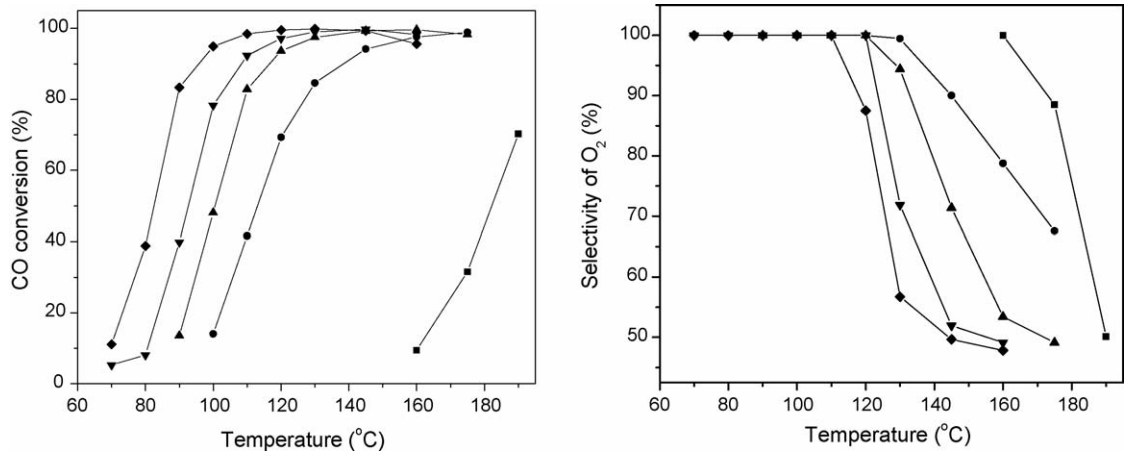

Fig. 4. The activity and selectivity of CuO–CeO_{2-x} catalysts prepared with different ratios of KOH/K_2CO_3, at a space velocity of 120,000 ml g^{-1} h^{-1} in a feed of 1% O_2, 1% CO, 50% H_2, Ar in balance, in the absence of CO_2 and H_2O: (■) 0:4, (●) 1:3, (▲) 2:2, (▼) 3:1, (♦) 4:0.

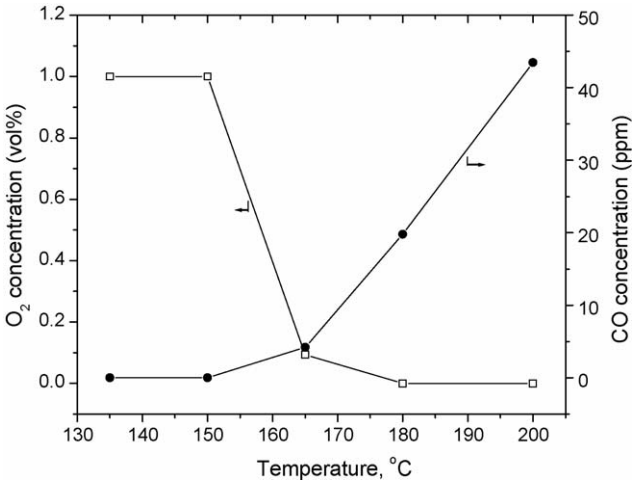

Fig. 5. The reverse water gas-shift reaction over the CuO–CeO_{2-x} catalyst with λ = 4:0. Reaction conditions: 50 mg of catalyst; feed gas of 1% O_2, 8% CO_2, 50% H_2 and Ar in balance; 120,000 ml g^{-1} h^{-1} of GHSV.

in the temperature range of performed kinetic experiments, and that no reverse WGS reaction is observed over the CuO–CeO_{2-x} catalyst at temperatures below 155 °C. The results show that the reverse water gas shift reaction has a slight influence on the selectivity and activity of the CuO–CeO_{2-x} catalyst at the temperatures lower than 160 °C. Therefore, the O_2 selectivity of 100% can be obtained over the CuO–CeO_{2-x} catalyst when reaction temperatures are lower than 120 °C, due to no competitive oxidation of H_2 and side reactions.

The influence of O_2/CO is depicted in Fig. 6. As shown in Fig. 6 (left), at a ratio of O_2/CO up to 0.75, the CO conversion shows a very weak dependence of the O_2/CO ratio. However, if the stoichiometric ratio of oxygen (O_2/CO = 0.5) is fed to the reactor in the presence of hydrogen, the CO reaches its maximum value (about 98%) at a temperature of 100 °C. At higher temperatures, the CO conversion curve lowers again. Correspondingly, the selectivity of O_2, seen in Fig. 6 (right), decreases as the increase in the O_2/CO ratio. Because more and more water is formed when O_2/CO ratio increases, oxygen more than the stoichiometric ratio is available for the H_2 oxidation reaction.

We also investigated the influence of space velocity, CO_2 and H_2O (seen in Fig. 7). According to literatures, both increase of

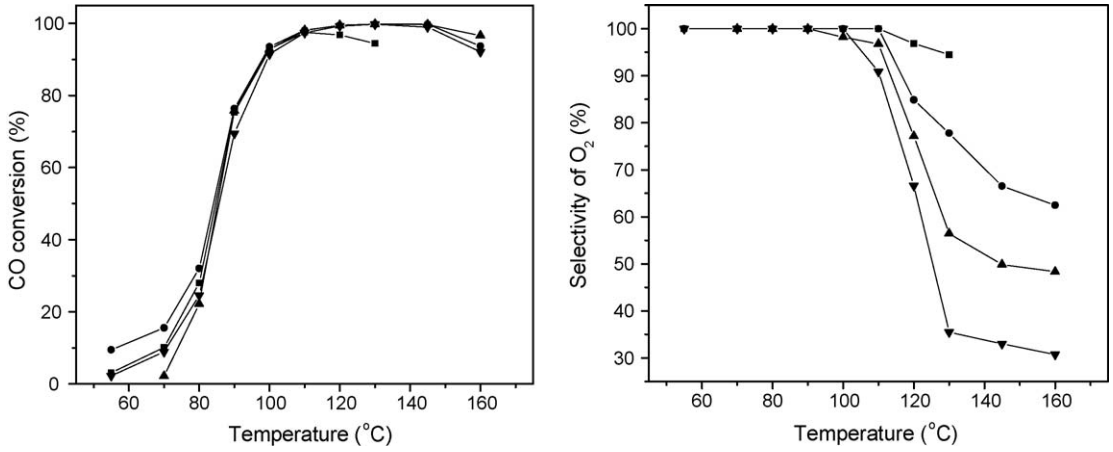

Fig. 6. The activity and selectivity of CuO–CeO_{2-x} catalysts prepared with the ratio of KOH/K_2CO_3 equal to 4:0, at a space velocity of 120,000 ml g^{-1} h^{-1}, in the absence of CO_2 and H_2O, O_2/CO = 0.5 (■), 0.75 (●), 1.0 (▲), 1.25 (▼).

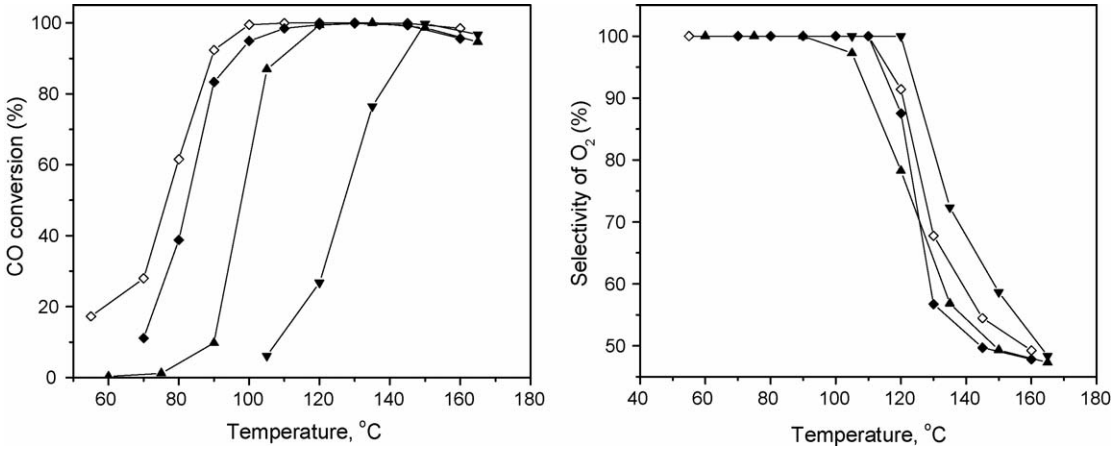

Fig. 7. The conversion of CO and selectivity of O_2 over CuO–CeO_{2-x} at a space velocity of 30,000 ml g^{-1} h^{-1} in the absence of CO_2 and H_2O (◊), at a space velocity of 120,000 ml g^{-1} h^{-1} in the absence of CO_2 and H_2O (♦), in the presence of CO_2 (▲), and in the presence of CO_2 and H_2O (▼).

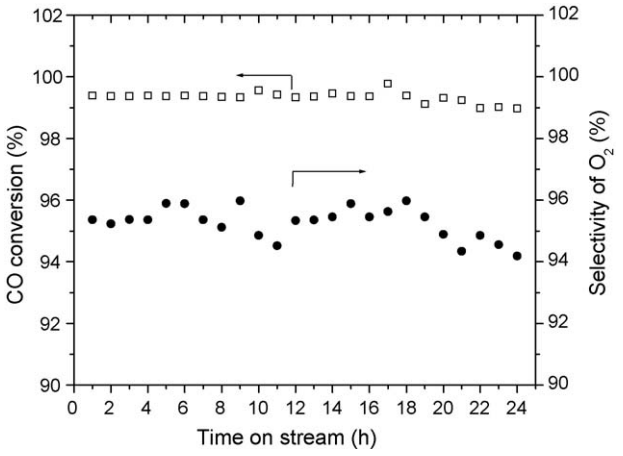

Fig. 8. Time on stream over the $CuO–CeO_{2-x}$ catalyst with λ = 4:0 at 120 °C. Reaction conditions: 50 mg of catalyst; feed gas of 1% O_2, 8% CO_2, 50% H_2 and Ar in balance; 120,000 ml g^{-1} h^{-1} of GHSV.

space velocity and addition of CO_2 and H_2O have a negative effect on the performance of $CuO–CeO_{2-x}$ catalysts. In the case of the space velocity of 120,000 ml g^{-1} h^{-1}, the curves of CO conversion and selectivity of O_2 over $CuO–CeO_{2-x}$ catalyst, in comparison with 30,000 ml g^{-1} h^{-1}, are slightly lower, as seen from both left and right images of Fig. 7. Similar trends can be seen for the addition of CO_2 and H_2O. The temperature with CO conversion of 99% in the presence of CO_2 or in the presence of CO_2 and H_2O is 120 and 150 °C, respectively. It is evident that the addition of CO_2 and H_2O depresses the performance of $CuO–CeO_{2-x}$ catalysts.

In order to investigate the stability of $CuO–CeO_{2-x}$ catalyst prepared with λ of 4:0, the duration test is run for 24 h at 120 °C and 120,000 ml g^{-1} h^{-1} of GHSV in a feed of 1% O_2, 1% CO, 50% H_2 and Ar in balance. As shown in Fig. 8, there is no obvious change in conversions of CO and selectivities of O_2 in the 24 h running test. CO conversions are kept at the values higher than 99% and selectivities of O_2 are kept at the values higher than 94% during the duration test. The result shows that the $CuO–CeO_{2-x}$ catalyst possesses a desirable stability, which is consistent with literatures [5,10].

4. Conclusions

The structural properties as well as the catalytic performance of $CuO–CeO_{2-x}$ catalysts have a strong dependence on precipitators. The BET, XRD and TPR results indicate that the addition of KOH as precipitators inhibits the growth of $CuO–CeO_{2-x}$ particles and yields nano-structured catalysts (d_{XRD} = 5.4–8.3 nm), increases the surface areas of $CuO–CeO_{2-x}$ catalysts from 39.9 to 138.0 m^2 g^{-1}. It is also find that the intensity of α peak in H_2-TPR of $CuO–CeO_{2-x}$ catalysts is in a good agreement with the oxidation performance of the $CuO–CeO_{2-x}$ catalysts. Namely, the catalyst prepared with λ of 4:0, maintaining the largest area of α peak, achieves the superior activity for the preferential oxidation of CO in rich hydrogen. CO conversion higher than 99% with O_2 selectivity of 100% can be obtained for this $CuO–CeO_{2-x}$ catalyst at 90–110 °C and a space velocity of 30,000–120,000 ml g^{-1} h^{-1} in the absence of CO_2 and H_2O or at 150 °C and a space velocity of 120,000 ml g^{-1} h^{-1} in the presence of CO_2 and H_2O.

Acknowledgment

The authors gratefully acknowledge the Ministry of Science and Technology of China (No. 2004 CB 719504).

References

[1] J. Kaspar, P. Fornasiero, J. Phys. Chem. B. 10 (1998) 557–561.
[2] N. Laosiripojana, S. Assabumrungrat, Appl. Catal. B: Environ. 60 (2005) 107–116.
[3] W. Liu, M. Flytzani-Stephanopoulos, Chem. Eng. J. 64 (1996) 283.
[4] G. Avgouropoulos, T. Loannides, H.K. Matralis, Catal. Lett. 73 (2001) 33.
[5] D.H. Kim, J.E. Cha, Catal. Lett. 86 (2003) 107.
[6] J.B. Wang, W.H. Shih, T.J. Huang, Appl. Catal. A: Gen. 203 (2000) 191–199.
[7] W. Liu, M. Flytzani-Stephanopoulos, J. Catal. 153 (1995) 304–316.
[8] D.H. Kim, J.E. Cha, Catal. Lett. 86 (1–3) (2003) 107–112.
[9] P.G. Harrison, I.K. Ball, W. Azelee, et al., Chem. Mater. 12 (2000) 3715–3725.
[10] G. Avgouropoulos, T. Ioannides, Appl. Catal. A: Gen. 244 (2003) 155–167.
[11] W. Shan, W. Shen, C. Li, et al., J. Catal. 228 (2004) 206–217.
[12] G. Avgouropoulos, T. Ioannides, H.K. Matralis, et al., Catal. Today 75 (2002) 157–167.
[13] G. Avgouropoulos, T. Loannides, H.K. Matralis, Catal. Lett. 73 (2001) 33.
[14] D.H. Kim, J.E. Cha, Catal. Lett. 86 (2003) 107.
[15] G. Marbán, A.B. Fuertes, Appl. Catal. B: Environ. 57 (2005) 43–53.
[16] W. Liu, M. Flytzani-Stephanopoulos, Chem. Eng. J. 64 (1996) 283.
[17] M. Luo, Y. Zhong, X. Yuan, X. Zheng, Appl. Catal. A: Gen. 162 (1997) 121.
[18] A.M. Arias, M.F. García, O. Gálvez, et al., J. Catal. 195 (2000) 207–216.